CEO Clinical and Experimental Otorhinolaryngology Vol. 19, No. 1: 55-69, February 2026
https://doi.org/10.21053/ceo.2025-00027
pISSN 1976-8710 eISSN 2005-0720

Original Article

Activation of the Gamma-Aminobutyric Acid (GABA)ergic Neural Circuit in Salicylate-Induced Tinnitus: the Inferior Colliculus to the Medial Geniculate Body

Xu-Yuan Peng[1,*] · Jiang Wang[1,*] · Ming-Yue Gong[1,*] · Li-Yuan Zhang[1] · Min Zhang[1]
Zhi-Bin Chen[1] · Zheng-Quan Tang[2,3] · Lei Cheng[1,4]

[1]*Department of Otorhinolaryngology and Hearing International Jiangsu Ear and Hearing Center, The First Affiliated Hospital with Nanjing Medical University, Nanjing, China*
[2]*School of Life Sciences, Anhui University, Hefei, China*
[3]*Key Laboratory of Human Microenvironment and Precision Medicine of Anhui Higher Education Institutes, Anhui University, Hefei, China*
[4]*Department of Allergology and Clinical Allergy Center, The First Affiliated Hospital with Nanjing Medical University, Nanjing, China*

Objectives. This study aimed to investigate the regulatory functions of gamma-aminobutyric acid (GABA)ergic neural circuits from the inferior colliculus (IC) to the medial geniculate body (MGB) in salicylate-induced tinnitus.

Methods. Mice were treated with salicylate to induce tinnitus, and tinnitus-like behaviors were evaluated via gap prepulse inhibition of acoustic startle. Using combined viral tracing methodologies, we identified and mapped the pathways and connections from the IC to the MGB. Furthermore, we employed Gq-coupled human M3 designer receptors exclusively activated by designer drugs (DREADDs) and Gi-coupled human M4 DREADDs to achieve targeted excitation or suppression of GABAergic neurons in the IC and MGB. Following the administration of clozapine N-oxide, which binds to these receptors, we modulated these neural circuits to assess their impact on tinnitus severity in a mouse model.

Results. Our findings demonstrated that mice exposed to salicylate exhibited tinnitus-like behaviors. GABAergic neurons projecting retrogradely from the MGB to the IC were primarily concentrated in the external nucleus of the IC. After clozapine N-oxide administration, chemogenetic activation of IC-MGB GABAergic neurons aggravated salicylate-induced tinnitus. Additionally, activation of GABAergic neurons between the IC and MGB induced the perception of tinnitus even without salicylate. However, chemogenetic inhibition of the IC-MGB GABAergic circuit did not reverse salicylate-induced tinnitus.

Conclusion. These findings suggest that activation of the IC-MGB GABAergic neural circuit may contribute to tinnitus generation through a mechanism distinct from that of salicylate-induced tinnitus. This study provides novel insights into the mechanisms underlying tinnitus.

Keywords. *Auditory Pathway; GABAergic; Inferior Colliculus; Medial Geniculate Body; Neural Circuit; Tinnitus*

• Received February 5, 2025
Revised July 1, 2025
Accepted July 6, 2025

• Corresponding author: **Lei Cheng**
Departments of Otorhinolaryngology and Allergology, The First Affiliated Hospital with Nanjing Medical University, 300 Guangzhou Rd, Nanjing 210029, China
Tel: +86-137-7662-0807, Fax: +86-25-8372-4440
Email: chenglei@jsph.org.cn

• Co-Corresponding author: **Zheng-Quan Tang**
School of Life Sciences, Anhui University, 111 Jiulong Rd, Hefei 230601, China
Tel: +86-181-1096-6646, Fax: +86-551-6386-1585
Email: zqtang@ahu.edu.cn

*These authors contributed equally to this work.

INTRODUCTION

Tinnitus is an auditory disorder characterized by abnormal perception without an external acoustic source, often experienced in the head or ears [1]. Tinnitus affects approximately 10% to 15% of adults, with consistently high prevalence across age groups [2]. Tinnitus may be associated with multiple factors, including hearing loss, ototoxic drugs, emotional stress, and sleep disturbances [3]. Consequently, tinnitus has emerged as a significant condition affecting both physical and mental health. Patients with tinnitus not only experience auditory stress but also face substantial interference with daily activities, impaired concentration, and disrupted sleep [1]. Moreover, tinnitus is linked to stress, emotional disturbances, and obsessive-compulsive tendencies, potentially leading to depression [4]. Thus, tinnitus poses a considerable challenge to both individuals and society. Although various therapeutic approaches have been investigated, current treatments are limited and primarily focus on symptom alleviation rather than complete resolution [5]. Therefore, understanding the mechanisms underlying tinnitus has become increasingly essential, highlighting the urgent need to explore its neurobiological foundations.

Previous studies have demonstrated that neurons across distinct brain areas exhibit heightened activity, particularly in key nuclei of the auditory pathway, such as the dorsal cochlear nucleus (DCN), inferior colliculus (IC), and medial geniculate body (MGB) [6]. Research has revealed hyperexcitability of the DCN in mice exhibiting tinnitus-related behaviors [7]. However, the DCN is considered to be primarily involved in the onset of tinnitus rather than its long-term maintenance [8]. The IC is essential for the initiation and continuation of tinnitus, and changes in its neurotransmitter activity are closely associated with the condition [9]. Tinnitus signals may be transmitted to the MGB via the IC. The primary role of the MGB is to integrate auditory information from the upstream auditory cortex (ACx) with downstream auditory and non-auditory signals [10]. The MGB gathers inputs from the IC and integrates gamma-aminobutyric acid (GABA) signals from the thalamic reticular nucleus (TRN), non-auditory signals from limbic regions such as the amygdala, and inputs from the ACx [11]. However, the role of the MGB in tinnitus pathology has often been overlooked. Recent studies using diffusion tensor imaging have shown reduced connectivity in the MGB of patients with tinnitus [12]. High-frequency stimulation of the MGB in rats alleviates tinnitus [13]. Additionally, deep brain stimulation targeting the MGB has demonstrated beneficial effects in tinnitus management [14]. Collectively, these studies suggest the MGB is crucial for the development and progression of tinnitus.

The MGB receives GABAergic afferents from the IC and TRN [15]. These GABAergic projections are essential for regulating auditory processing within the MGB, and normal MGB function depends on GABAergic inhibition [16]. Tinnitus-associated thalamocortical hyperactivity and abrupt changes in the ACx may result in the upregulation or downregulation of inhibitory functions within the MGB [17]. Findings regarding MGB GABAergic dysfunction in tinnitus are somewhat contradictory. Some researchers have reported that mice with salicylate-induced tinnitus exhibit altered excitability and inhibition in the MGB [18]. Another study indicated that a frequency-nonspecific reduction in frequency tuning selectivity begins at the level of the MGB, implying that tinnitus may be associated with decreased inhibitory control via the auditory pathway [19]. GABA sensitivity is greater in the MGB than in the IC and is potentially modulated by both high-affinity extrasynaptic and synaptic components. This heightened sensitivity to GABA may be fundamental to the auditory thalamus's crucial filtering function in processing incoming sound information, a phenomenon possibly linked to the thalamocortical dysrhythmia (TCD) hypothesis [20]. GABAergic neurons constitute a substantial proportion (20%–40%) of neurons projecting from the IC to the auditory thalamus [21]. However, it remains uncertain whether the IC and MGB interact to regulate tinnitus. Here, we investigated the role of the GABAergic IC-MGB neural circuit in tinnitus.

This study employed viral tracing and immunofluorescence confocal imaging to characterize projections from the IC to the MGB, aiming to elucidate the underlying circuit mechanisms. By using Gq-coupled human M3 designer receptors exclusively activated by designer drugs (hM3Dq DREADDs) and Gi-coupled human M4 designer receptors also exclusively activated by designer drugs (hM4Di DREADDs), we investigated the role of the IC-MGB GABAergic neural circuit in salicylate-induced tinnitus. Exploring the mechanism of action of this neural circuit in tinnitus may aid in identifying better treatment targets.

HIGHLIGHTS

- Activation of the inferior colliculus (IC)-medial geniculate body (MGB) gamma-aminobutyric acid (GABA)ergic neural circuit may contribute to tinnitus generation.
- Activation of the IC-MGB GABAergic neural circuit elevates c-Fos levels in the auditory cortex.
- This study explores the IC-MGB circuit in tinnitus via viral tracing and chemogenetic methods.

MATERIALS AND METHODS

Experimental design rationale and overview

To systematically investigate the role of the IC-MGB GABAergic neural circuit in salicylate-induced tinnitus, this study employed a multi-step experimental design. First, adeno-associated virus (AAV)-based stereotactic injections were performed in C57/BL 6J and Vgat-Cre mice (detailed in section "Animals") to map the

anatomical projections of the circuit (virus details in section "Stereotaxic surgery and virus injection"). Second, the C57/BL 6J mice were used to establish a salicylate-induced tinnitus model. After intraperitoneal injection of salicylate, tinnitus was assessed via gap prepulse inhibition of the acoustic startle (GPIAS) reflex (detailed in section "Behavioral test"). Mice were then divided into two groups: the experimental group (n=8) received rAAV-Ef1α-DIO-hM3D(Gq)-mCherry-WPREs, and the control group (n=6) received rAAV-EF1α-DIO-mCherry-WPRE-hGHpolyA (detailed in section "Stereotaxic surgery and virus injection"). Three weeks later, clozapine N-oxide (CNO) was injected to activate the circuit, followed by GPIAS-based behavioral assessment. Next, to determine if circuit activation directly induces tinnitus perception, the above viral injection protocol was repeated in new experimental (n=8) and control (n=5) groups. Finally, to explore the role of circuit inhibition, C57/BL 6J mice were modeled using salicylate and evaluated by GPIAS. The experimental group (n=8) was injected with rAAV-Ef1α-DIO-hM4D(Gi)-mCherry-WPREs, while the control group (n=5) received rAAV-EF1α-DIO-mCherry-WPRE-hGHpolyA. After 3 weeks, CNO was administered to inhibit the circuit, and behavioral changes were monitored via GPIAS.

Animals

C57BL/6J male mice (7–10 weeks of age, 20–25 g) were obtained from Hangzhou Ziyuan Laboratory Animal Technology Co., Ltd. Age-matched male Vgat-IRES-Cre mice were purchased from Cyagen. The mice were maintained in a clean and ventilated standard animal facility, which housed four per cage in a 12-hour light/dark cycle, with illumination from 7 AM to 7 PM and a controlled environment (21 °C–23 °C ambient temperature and humidity-controlled 40%–70%). A designated individual was tasked with routine cleaning of the animal cages, replacement of bedding, and regular provision of fresh food and water. Before the experiment, experimental mice were confirmed to have normal hearing via the auditory brainstem response (ABR). All animal research and experimental protocols were approved by the Animal Care and Use Committee of the Animal Facility at Anhui University (No. 2020-039).

Stereotaxic surgery and virus injection

After anesthetization with sodium pentobarbital, the mice underwent stereotaxic surgery, during which the incisors and both sides of the head were fixed on a special mouse stereotaxic frame (RWD). The core temperature was sustained at 36 °C with the aid of a heating pad during the procedure. Medical eye ointment was placed over both eyes of each mouse to prevent eye drying. The connective tissue on the cranial surface was removed using a hydrogen peroxide solution to sufficiently expose the cranial surface for observation. The stereotaxic apparatus was subsequently adjusted according to the relative positions of the anterior and posterior fontanelles to ensure that the mouse brain was flushed in the horizontal plane. After the above steps were completed, the experimental target brain regions were localized, and holes were drilled at the corresponding locations in the skull for virus injection. In accordance with the experimental design, either 200–300 nL of the virus was administered at a flow rate of 50 nL/min via a 10 mL syringe needle (Hamilton). After the infusion was completed, the syringe was held in the dorsal-ventral coordinates for 5 minutes to enable viral dissemination, after which the pipette was left undisturbed for an additional 10 minutes prior to its removal. After surgery, mice were housed in a suitable environment for recovery and provided with adequate food and water. To ensure effective viral expression and complete recovery of the mice, behavioral tests should be scheduled at least 3 weeks after the completion of surgery, which also ensures that the experimental data are reasonable and accurate.

For anatomical-tracing experiments, rAAV-EF1α-DIO-mCherry-WPRE-hGH polyA (5.18E+12 v.g/mL) was injected at multiple volumes (200 nL) into the IC of Vgat-IRES-Cre animals (anterior-posterior from the bregma [A/P], –4.60 mm; medial-lateral from the midline [M/L], ±1.20 mm; dorsal-ventral from the brain surface [D/V], –1.10 mm) bilaterally. rAAV-Ef1α-DIO-mCherry-WPREs (5.18E+12 v.g/mL) was injected at multiple volumes (200 nL) into the IC, and rAAV(Retro)-Vgat-Cre-WPRE-hGH polyA, AAV2/R (5.04E+12 v.g/mL) was injected at multiple volumes (200 nL) into the MGB (A/P, –3.0 mm; M/L, ±2.0 mm; D/V, –3.0 mm) bilaterally in C57BL6/J mice. The animals underwent a 3-week recovery period to facilitate maximum viral expression, after which they were prepared for immunohistochemical experiments.

For chemogenetic manipulation experiments, rAAV-Ef1α-DIO-hM3D(Gq)-mCherry-WPREs (5.26E+12 v.g/mL), rAAV-Ef1α-DIO-hM4D(Gi)-mCherry-WPREs (5. 25E+12 v.g/mL), rAAV-EF1α-DIO-mCherry-WPRE-hGH polyA (5.18E+12 v.g/mL), rAAV(Retro)-Vgat-Cre-WPRE-hGH polyA, AAV2/R (5.04E+12 v.g/mL) were used. The formers were injected at multiple volumes (300 nL) into the IC (A/P, –4.60 mm; M/L, ±1.20 mm; D/V, –1.10 mm) bilaterally and latter was injected at multiple volumes (300 nL) into the MGB (A/P, –3.0 mm; M/L, ±2.0 mm; D/V, –3.0 mm) bilaterally in C57BL6/J mice. The animals received a minimum recovery time of 3 weeks to achieve optimal viral expression. CNO (1 mg/kg, initially dissolved in dimethyl sulfoxide and subsequently diluted in NaCl to reach a final concentration of 100 μg/mL) was administered intraperitoneally 30 minutes before the behavioral experiments. All viruses and CNO were obtained from BrainVTA.

Behavioral test

The startle reflex was elicited by a strong acoustic stimulus. However, a short silent gap inserted before the strong acoustic stimulus in the ongoing background noise diminishes the startle response. In animals with tinnitus, the inhibitory effect of the silent gap diminished when the background noise resembled a tinnitus sound.

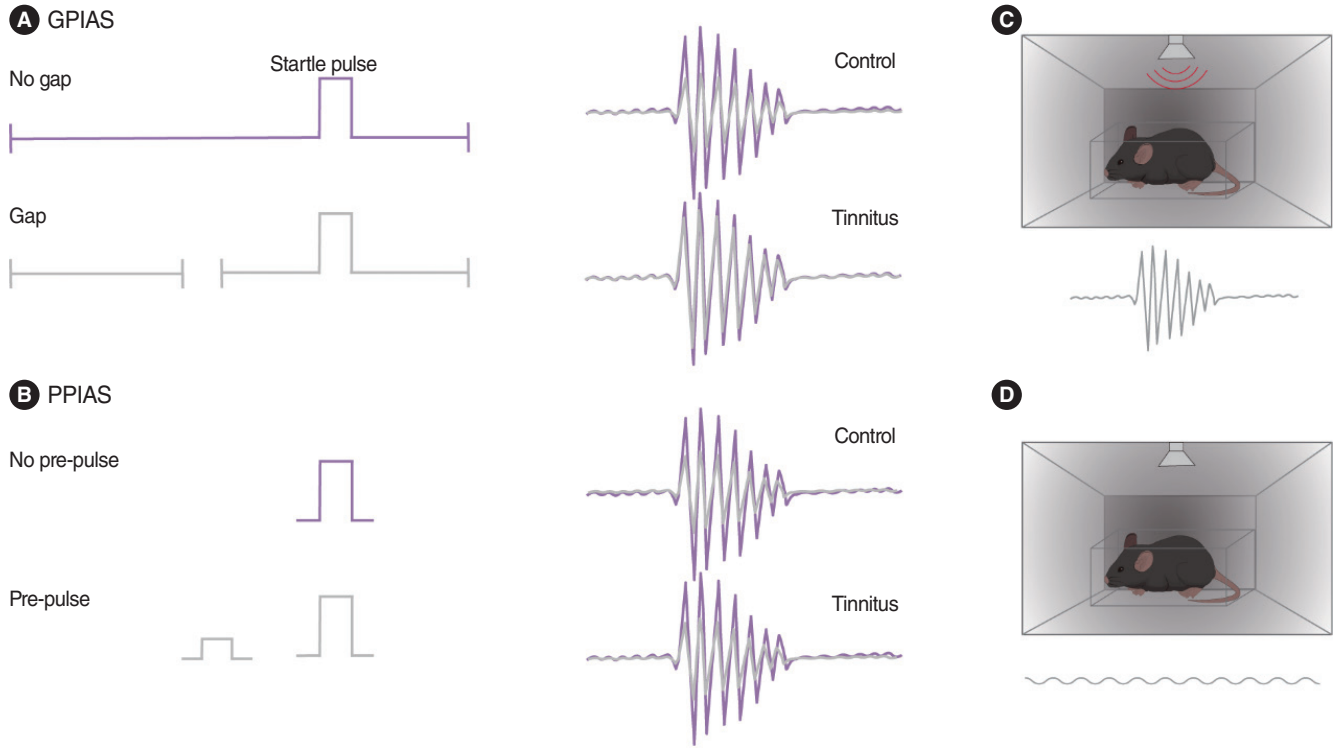

Fig. 1. Schematic of the tinnitus startle reflex model. (A) Diagram illustrating the gap prepulse inhibition of the acoustic startle (GPIAS) protocol. (B) Diagram illustrating the prepulse inhibition of acoustic startle (PPIAS) protocol. (C) Diagram illustrating mice subjected to sound stimulation. (D) Diagram illustrating mice not subjected to sound stimulation.

Gap detection was tested through a startle stimulus presented through a loudspeaker positioned 15 cm above the animal's head, which emitted the sound stimulus. Startle amplitude measurements were performed using a pressure-sensing collector located at the bottom end of the mouse. Each group of mice was placed in the device for 10 minutes on four consecutive days for acclimatization before the start of the formal experiment. The test equipment was cleaned with 70% ethanol to eliminate odors from the mice before and after each experiment.

Gap prepulse inhibition of acoustic startle (GPIAS) (Fig. 1A and C): the background signal in the startle chamber consisted of 8, 12, 16, 20, 24, and 32 kHz of 70 dB narrowband noise, and the startle stimulus was 20 ms of 110 dB white noise. In the gap trials, a silent interval of 50 ms was introduced 130 ms before the start of the startle stimulus. Each testing session consisted of 20 trials, with half featuring a silent gap and the other half lacking it, all presented at variable stimulus intervals ranging from 20 to 25 seconds. Before each test, each mouse underwent a 5-minute acclimation in a startle chamber, followed by 20 stimulus trials to familiarize them with the startle reflex. A complete trial (including all frequencies) lasted approximately 60 minutes. The main test index in the GPIAS was the degree of inhibition of the startle reflex by the auditory startle interval pre-stimulus, gap startle ratio=gap/no gap (where gap indicates the peak-to-trough difference evoked when there is a gap as a pre-stimulus, and no gap indicates the peak-to-trough difference evoked when there is no gap).

Prepulse inhibition of acoustic startle (PPIAS) (Fig. 1B and D): the parameters of the acoustic stimulus signal for the startle reflex were identical to those in the GPIAS test. The acoustic stimulus signal that appeared alone (no prepulse group) or a weak stimulus (narrow-band noise, 70 dB, six different frequencies: 8, 12, 16, 20, 24, and 32 kHz; duration: 50 ms) was given 130 ms before the acoustic stimulus signal without eliciting a startle reflex (prepulse group). Each test consisted of 20 trials, half with including and half excluding a prepulse, presented at a randomly variable stimulus interval of 20–25 seconds. The primary index evaluated in PPIAS was the extent to which the prepulse diminished the acoustic startle reflex. PPI startle ratio=prepulse/no prepulse (where prepulse denotes the difference in peaks and valleys evoked with prepulse stimulation, and no prepulse denotes the difference in peaks and valleys evoked without prepulse suppression). Data were processed using MATLAB 2016a scripts developed in-house.

ABR recording

To evaluate the effects of the experimental procedures, auditory function was assessed by measuring ABR in mice. These recordings were conducted before and after the completion of the experimental protocols to track potential changes in auditory sen-

sitivity. Using the RZ6 platform (TDT), ABR recordings were conducted in a soundproof chamber while the animals were anesthetized with pentobarbital sodium (40 mg/kg) and maintained at a stable temperature via a regulated heating device. The soundproof room was designed to meet the requirements of the acoustic experiments, effectively isolating external noise interference, thus ensuring the accuracy of the ABR recordings. Three electrodes were inserted into the back of one auricle (reference electrode), the top of the head (subdermal needle electrode), and contralateral hind leg (grounding electrode). The stimulus signal consisted of a click (10 ms, 22 times/sec) and a tone burst, where the tone bursts were centered at 8, 12, 16, 20, 24, and 32 kHz, and a rise/fall time of 0.5 ms was used to create a smooth sound waveform. The starting sound pressure level (SPL) was set to 90 dB, which was decreased in 10 dB increments until the evoked response waveform ceased. The hearing threshold was determined by analyzing the ABR waveform and marking it as the minimum sound level of the arousal response waveform (especially waves I and II).

Immunohistochemistry and imaging

Upon completion of the experimental procedures, the animals received terminal anesthesia via the intraperitoneal delivery of pentobarbital sodium (40 mg/kg). Transcardiac perfusion was then performed, first administering 20 mL of 0.01 M phosphate-buffered saline (PBS), followed by fixation with 20 mL of 4% paraformaldehyde (PFA). Following the perfusion procedure, brain tissue was extracted and underwent overnight fixation in 4% PFA at 4 °C. Tissue preservation continued with immersion in 30% sucrose solution (prepared in 0.01 M PBS) at 4 °C, maintained for a 3-day period. Brains containing the IC, MGB, and ACx were sectioned into coronal slices (40 μm) on a cryostat microtome (RWD FS800) and harvested for immunofluorescence.

For immunofluorescence staining, sections were initially rinsed in 0.01 M PBS with three 10-minute washes. To minimize background interference and enhance staining specificity, the tissues were subjected to a blocking solution (5% BSA and 0.5% Triton X-100 in PBS) under ambient conditions for 1 hour. Subsequently, the brain sections were exposed to antigen-specific primary antibodies, with incubation carried out overnight (20 hours) under refrigerated conditions (4 °C). Immunolabeling was performed using two key antibodies: antibodies against GABA (1:500, A2052, rabbit; Sigma Aldrich) and anti-c-Fos (1:2,400, 2,250, rabbit; Cell Signaling). After rinsing with PBS rinses (0.01 M, three times), the brain sections underwent a 2-hour fluorescent labeling step at ambient temperature using species-matched secondary detection reagents. Secondary antibodies used were Alexa Fluor 488-anti-rabbit (1:500, A24221; Abbkine Scientific) and Alexa Fluor 594-anti-rabbit (1:500, A24421; Abbkine Scientific). After washing again in PBS, all the brain slices were processed for fluorescence staining with DAPI Fluoromount-G (Cat# BMU107-CN; Abbkine), fixed, and prepared with a coverslip for visualization. Fluorescence signals from the specimens were analyzed and recorded using a confocal microscope (SpinSR, Olympus), PanoBrain, and Meca Scientific and further analyzed using ImageJ software.

Statistical analysis

Statistical analyses and graph generation were performed using GraphPad Prism version 9.5.0. The Shapiro-Wilk test was used to assess the normal distribution of the data. When comparing groups with more than two datasets, a two-way analysis of variance was performed, accompanied by a Bonferroni post-hoc adjustment for multiple comparisons. All the data were represented as the means±standard errors of the means, with statistical significance indicated by $P<0.05$, $P<0.01$, $P<0.001$, and $P<0.0001$.

RESULTS

Inhibitory IC-MGB GABAergic neural circuit

We injected an anterograde monosynaptic rAAV-EF1α-DIO-mCherry-WPRE-hGHpolyA virus into the IC of Vgat-Cre mice. After 3 weeks, the MGB showed neurons positive for red fluorescent protein (mCherry$^+$) (Fig. 2A-C), and mCherry predominantly co-localized with a GABA-specific antibody in the IC (Fig. 2D). To further confirm IC-MGB GABAergic projection, the rAAV-EF1α-DIO-mCherry-WPRE-hGHpolyA virus was injected into the IC, and a retro-AAV containing the *Vgat1* promoter and Cre element (rAAV(Retro)-Vgat1-Cre) was injected into the MGB of C57BL/6J mice. Immunohistochemical staining revealed mCherry-positive neurons co-localized with the GABA-specific antibody (Fig. 2E-H). These results indicate the involvement of the IC-MGB GABAergic pathway.

Chemogenetic activation of IC^{GABA} neurons in the IC-MGB neural circuit aggravated tinnitus perception in mice with salicylate-induced tinnitus

One week before viral expression, we induced tinnitus by administering a salicylate injection (350 mg/kg). Tinnitus was detected using a startle reflex protocol, allowing us to confirm its development after salicylate injection. The experimental procedure is illustrated in Fig. 3A. Before tinnitus testing, the mice underwent 4 days of acclimatization to the testing environment to eliminate environmental influences, followed by GPIAS testing and baseline tests for PPIAS. Next, we used a chemogenetic approach to selectively express Gq-DREADD in IC^{GABA} neurons by injecting AAV-DIO-hM3Dq-mCherry (Gq-DREADD) into the IC and rAAV(Retro)-Vgat1-Cre into the MGB of C57BL/6J mice (Fig. 3B and C). Immunohistochemical staining showed that mCherry-positive neurons co-localized with a GABA-specific antibody (Fig. 3D).

Intraperitoneal injection of salicylate was conducted 1 week before full viral expression, and GPIAS was performed to assess

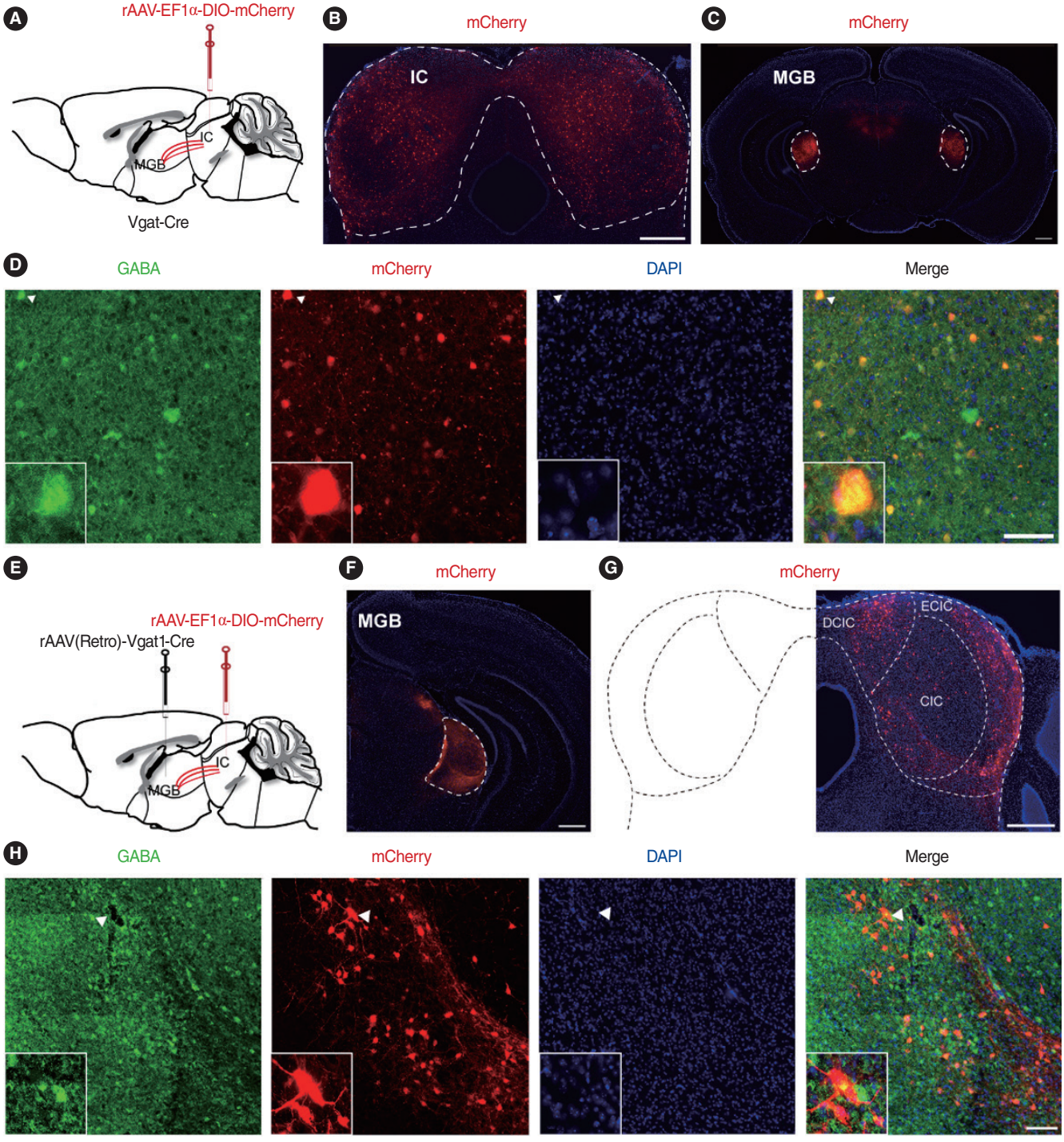

Fig. 2. IC^{GABA} neurons projecting to the medial geniculate body (MGB). (A) Schematic depicting anterograde tracing. (B) Representative image of mCherry-expressing neurons in the inferior colliculus (IC). Scale bar, 500 μm. (C) Representative image of mCherry-expressing neurons in the MGB. Scale bar, 500 μm. (D) Characterization of mCherry-positive IC neurons; these neurons are reactive with gamma-aminobutyric acid (GABA)-specific antibody. Scale bars, 100 μm. (E) Schematic depicting retrograde tracing. (F) Representative image of mCherry-expressing neurons in the MGB. Scale bar, 500 μm. (G) Representative image of mCherry-expressing neurons in the IC. Scale bar, 500 μm. (H) Characterization of mCherry-positive IC neurons; these neurons are reactive with GABA-specific antibody. The arrowheads indicate the co-localized neurons labeled by different fluorescent signals (for GABA, mCherry, and DAPI). Scale bars, 100 μm. DAPI, 4′,6-diamidino-2-phenylindole; CIC, central nucleus of the inferior colliculus; DCIC, dorsal cortex of the inferior colliculus; ECIC, external cortex of the inferior colliculus.

tinnitus. The results indicated notable differences in the hM3Dq-mCherry mouse group (n=8) at 8 and 20 kHz on day 7 after salicylate injection (Fig. 3E), confirming tinnitus at these two frequencies. Similarly, a notable difference was observed in the mCherry group (n=6) at 8 and 16 kHz (Fig. 3F), indicating tinnitus at these frequencies. Next, the IC-MGB circuit was activated by intraperitoneal injection of CNO (1 mg/kg), followed by GPIAS tests performed 30 minutes later. After chemogenetic activation, mice treated with hM3Dq-mCherry exhibited increased levels of tinnitus at 8 kHz and 20 kHz. Interestingly, a frequency that was previously tinnitus-free (12 kHz) also displayed tinnitus after activation (Fig. 3G). The mCherry group did not exhibit aggravated tinnitus at the corresponding frequencies (Fig. 3H). Additionally, no significant differences in PPIAS were observed, indicating that GPIAS results in both experimental and control mice were not due to temporal processing deficits or difficulties in detecting background noise (Fig. 3I and J). ABR data demonstrated that the observed changes in GPIAS were not attributable to salicylate-induced hearing loss (Supplementary Fig. 1).

Chemogenetic activation of IC^{GABA} neurons in the IC-MGB neural circuit induced tinnitus perception

We performed direct chemogenetic activation of this circuit in the absence of salicylate. The experimental procedure is shown in Fig. 4A. As in the previous experiment, we selectively expressed Gi-DREADD in IC^{GABA} neurons using a chemogenetic approach by injecting AAV-DIO-hM3Dq-mCherry (Gq-DREADD) into the IC and rAAV(Retro)-Vgat1-Cre into the MGB of C57BL/6J mice (Fig. 4B). To confirm whether chemogenetic manipulation successfully activated the IC-MGB GABAergic pathway, we evaluated the expression of the neuronal activation protein c-Fos. The findings indicated a significant increase in c-Fos expression in the IC of the experimental group relative to the control group (Fig. 4C), indicating effective activation of the IC-MGB GABAergic neural circuit. Upon intraperitoneal administration of CNO, chemogenetic manipulation was found to induce tinnitus at 8, 12, and 20 kHz in the hM3Dq-mCherry group (Fig. 4D), whereas no significant change was observed in the mCherry group (Fig. 4E). Similarly, the PPIAS (Fig. 4F and G) and ABR test results (Supplementary Fig. 2) did not differ significantly between the hM3Dq-mCherry and mCherry mice, indicating that the GPIAS test results were not affected by time or hearing.

Chemogenetic inhibition of IC^{GABA} neurons in the IC-MGB neural circuit had no effect on tinnitus in salicylate-injected mice

The IC-MGB GABAergic neural circuit was inhibited in salicylate-induced tinnitus. The experimental flowchart is presented in Fig. 5A. After measuring baseline levels of GPIAS and PPIAS, we selectively expressed Gi-DREADD in IC^{GABA} neurons using a chemogenetic approach by injecting AAV-DIO-hM4Di-mCherry (Gi-DREADD) into the IC and rAAV(Retro)-Vgat1-Cre into the MGB of C57BL/6J mice (Fig. 5B and C). Immunohistochemical staining demonstrated that mCherry-positive neurons co-localized with a GABA-specific antibody (Fig. 5D). Salicylate was injected the day before CNO injection to induce tinnitus. After salicylate injection, hM4Di-mCherry and mCherry mice exhibited notable differences at frequencies of 8 and 16 kHz (Fig. 5E and F), indicating that tinnitus was induced at these frequencies. Subsequently, CNO was injected intraperitoneally 30 minutes before the behavioral assessment to inhibit the IC-MGB GABAergic circuit. We found that tinnitus levels in the hM4Di-mCher-

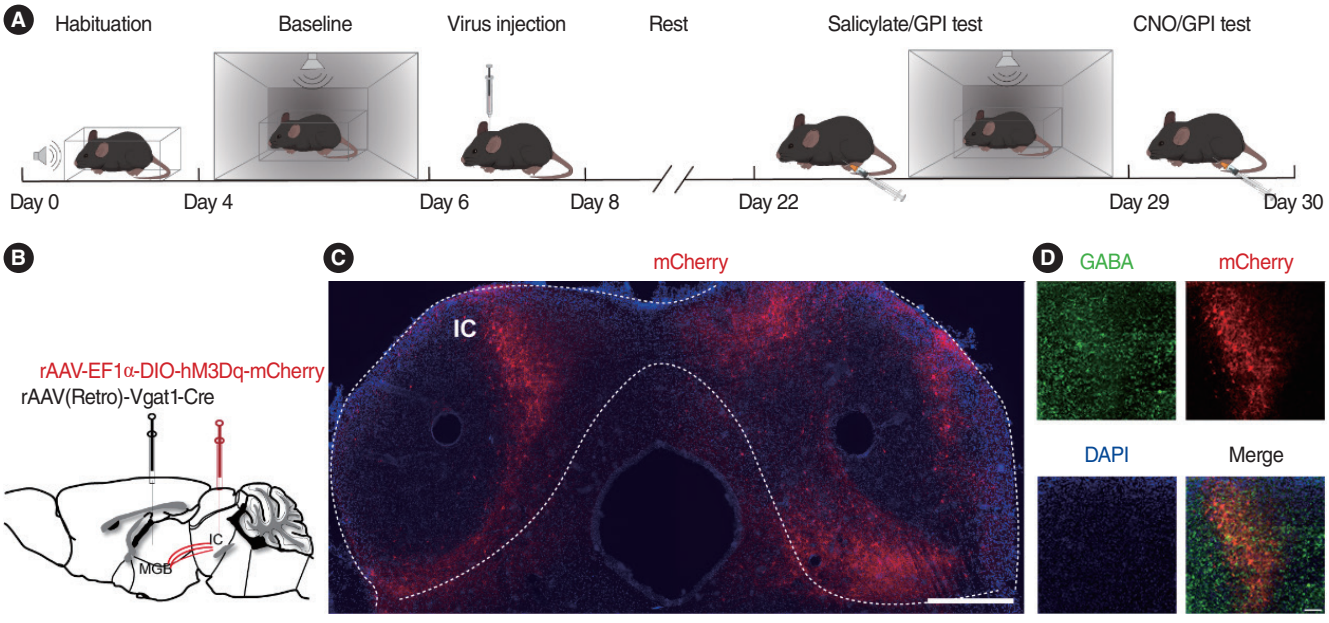

Fig. 3. Continued

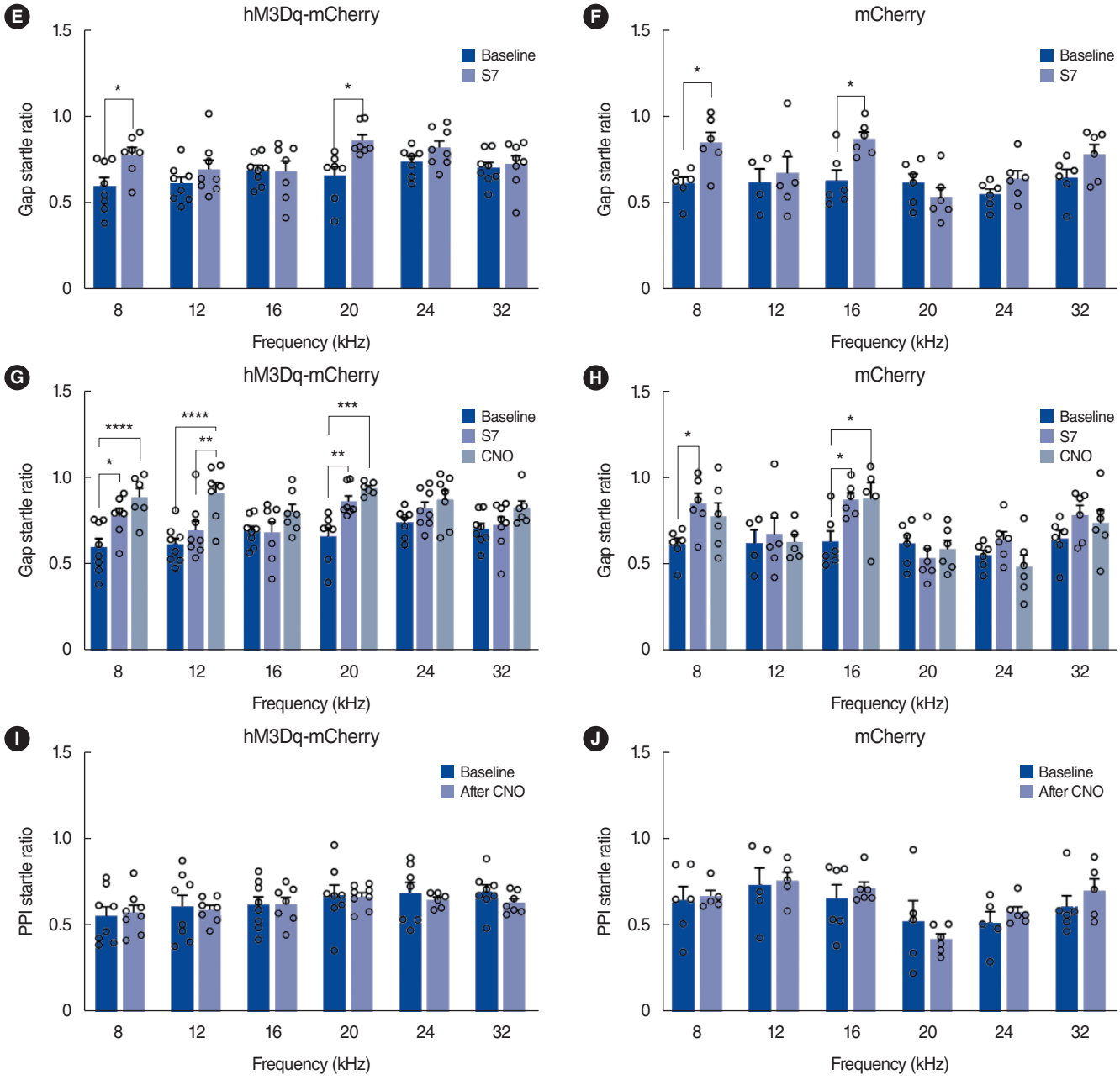

Fig. 3. Chemogenetic activation of IC^{GABA} neuron activity in the inferior colliculus (IC)-medial geniculate body (MGB) neural circuit in salicylate-induced tinnitus. (A) Timeline of the experiments. (B) Schematic of viral injection for chemogenetic manipulations. (C) Representative image of mCherry-expressing neurons in the IC. Scale bar, 500 μm. (D) Characterization of mCherry-positive IC neurons; these neurons are reactive with gamma-aminobutyric acid (GABA)-specific antibody. Scale bars, 100 μm. (E, F) Gap startle ratios across various frequencies in mice injected with salicylate. (E) Column factor, F(1,79)=13.41, P=0.001; hM3Dq-mCherry: 8 kHz, 95% CI: −0.355 to −0.010, P=0.032; 20 kHz, 95% CI: −0.384 to −0.0282, P=0.015. (F) Column factor, F(1,58)=11.37, P=0.001; mCherry: 8 kHz, 95% CI: −0.457 to −0.018, P=0.027; 16 kHz, 95% CI: −0.465 to −0.027, P=0.020. (G, H) Gap startle ratios across various frequencies in mice injected with clozapine N-oxide (CNO). (G) Column factor, F(2,112)=29.51, P<0.001; hM3Dq-mCherry: 8 kHz_baseline vs. 8 kHz_S7, 95% CI: −0.335 to −0.030, P=0.015; 8 kHz_baseline vs. 8 kHz_CNO, 95% CI: −0.450 to −0.132, P<0.001; 12 kHz_baseline vs. 12 kHz_CNO, 95% CI: −0.455 to −0.150, P<0.001; 12 kHz_S7 vs. 12 kHz_CNO, 95% CI: −0.372 to −0.068, P=0.002; 20 kHz_baseline vs. 20 kHz_S7, 95% CI: −0.363 to −0.049, P=0.007; 20 kHz_baseline vs. 20 kHz_CNO, 95% CI: −0.448 to −0.121, P=0.0002. (H) Column factor, F(2,86)=4.917, P=0.010; mCherry: 8 kHz_baseline vs. 8 kHz_S7, 95% CI: −0.445 to −0.030, P=0.021; 16 kHz_baseline vs. 16 kHz_S7, 95% CI: −0.454 to −0.039, P=0.016; 16 kHz_baseline vs. 16 kHz_CNO, 95% CI: −0.469 to −0.034, P=0.019. (I, J) Prepulse inhibition (PPI) startle ratios across various frequencies in mice. (I) PPI startle ratios of the hM3Dq-mCherry group. (J) PPI startle ratios of the mCherry group. Values are presented as mean±standard error of the mean. *P<0.05, **P<0.01, ***P<0.001, ****P<0.0001 (two-way analysis of variance for E-J). hM3Dq-mCherry, n=8 mice; mCherry, n=6 mice. GPI, gap prepulse inhibition; DAPI, 4′,6-diamidino-2-phenylindole; S7, salicylate day 7.

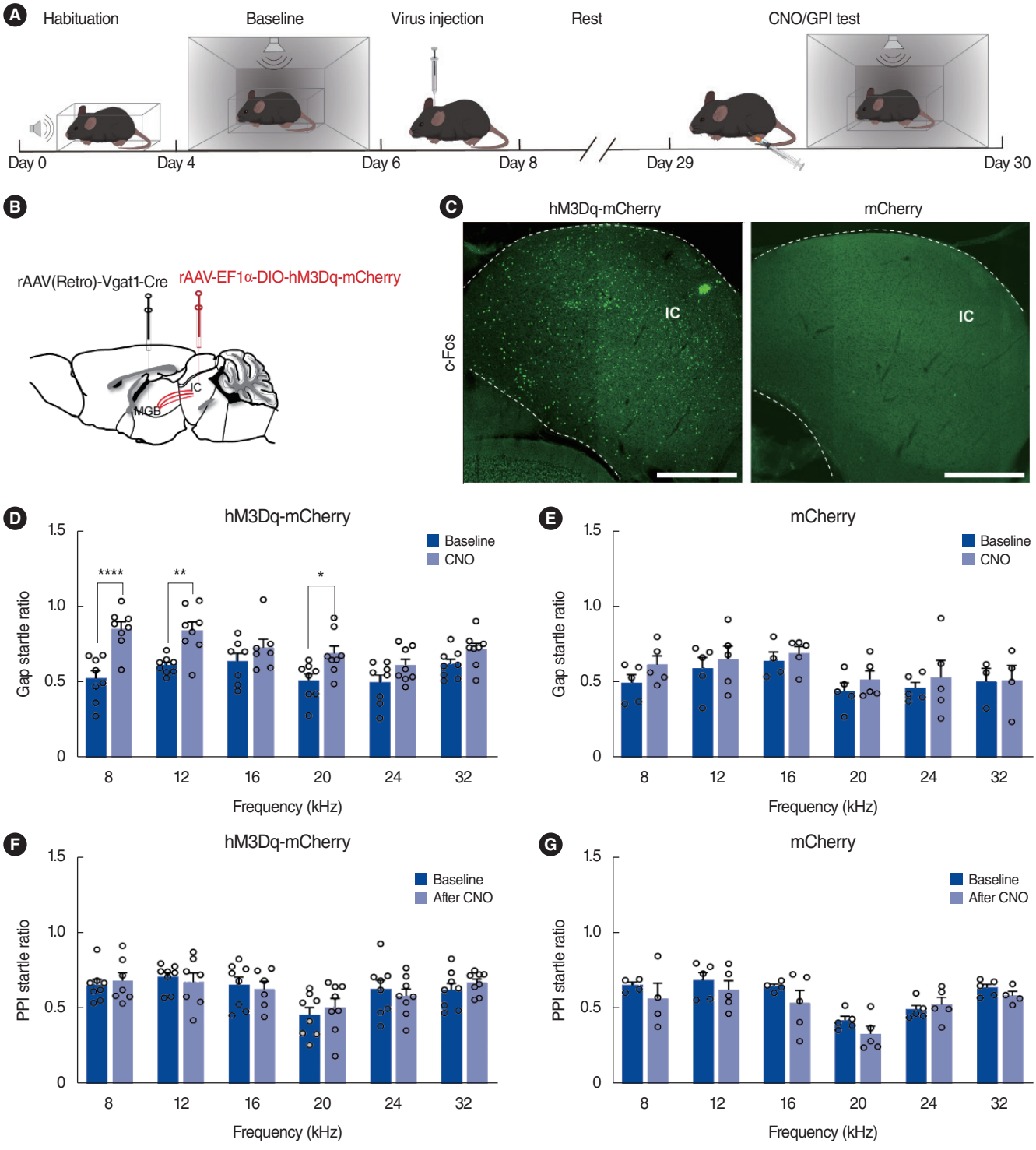

Fig. 4. Chemogenetic activation of inferior colliculus (IC) gamma-aminobutyric acid (GABA)ergic neuron activity in the IC-medial geniculate body (MGB) neural circuit. (A) Timeline of the experiments. (B) Schematic illustration of viral injection for chemogenetic manipulation. (C) c-Fos expression in the IC of mice with the IC-MGB neural circuit expressing hM3Dq-mCherry/mCherry following clozapine N-oxide (CNO) injection. Scale bars, 500 μm. (D, E) Gap startle ratios across various frequencies in mice injected with CNO. (D) Column factor, $F(1,82)=41.70$, $P<0.001$; hM3Dq-mCherry: 8 kHz, 95% CI: −0.506 to −0.155, $P<0.001$; 12 kHz, 95% CI: −0.408 to −0.056, $P=0.004$; 20 kHz, 95% CI: −0.356 to −0.004, $P=0.042$. (E) Gap startle ratios of the mCherry group. (F, G) Prepulse inhibition (PPI) startle ratios across various frequencies in mice. (F) PPI startle ratios of the hM3Dq-mCherry group. (G) PPI startle ratios of the mCherry group. Values are presented as mean±standard error of the mean. *$P<0.05$; **$P<0.01$; ****$P<0.0001$ (two-way analysis of variance for D-G). hM3Dq-mCherry, n=8 mice; mCherry, n=5 mice. GPI, gap prepulse inhibition.

ry and mCherry groups did not change significantly before and after CNO injection (Fig. 5G and H), and their PPIAS values were not significantly different (Fig. 5I and J). ABR thresholds confirmed the observed changes in GPIAS (Supplementary Fig. 3).

Chemogenetic activation of the IC-MGB significantly elevated c-Fos levels in the ACx relative to control mice

Finally, to verify whether chemogenetic activation of the IC-MGB GABAergic circuit induces tinnitus, we stained the ACx brain regions of mice from the previous two experiments with c-Fos. Compared with the control group, both the salicylate+hM3Dq and hM3Dq groups exhibited increased c-Fos levels in the ACx (Fig. 6), confirming that activation of the IC-MGB can induce tinnitus.

DISCUSSION

This study established the critical role of the IC-MGB GABAergic neural circuit in tinnitus perception. We verified the GABAergic neural circuit connections from the IC to the MGB using anterograde and retrograde viral tracing techniques. Moreover, we manipulated the IC-MGB GABAergic neural circuit through chemogenetic modulation and observed corresponding changes in tinnitus perception and generation before and after CNO injection. Our findings indicated that chemogenetic activation of this neural circuit induces tinnitus and exacerbates the severity of salicylate-induced tinnitus. However, chemogenetic inhibition of this circuit did not significantly influence tinnitus.

Salicylate-induced auditory dysfunction involves both peripheral and central nervous system mechanisms [22,23]. Salicylate alters outer hair cell structure and inhibits cyclooxygenase activity in the cochlea, potentially contributing to the development of tinnitus [24-26]. Salicylate can easily cross the blood-brain barrier and reach concentrations of 1–2 mM in the cerebrospinal fluid, which are sufficient to inhibit $GABA_A$ receptor currents [27,28]. Additionally, cortical hyperactivity—a feature of neural plasticity associated with tinnitus—may be triggered at these concentrations [28,29]. Furthermore, salicylate administration activates the Ca^{2+}/CaMKII/CREB signaling pathway in ACx cells, potentially intensifying the perception of tinnitus [30]. However, the exact mechanism of salicylate-induced tinnitus remains unclear.

In this study, we used viral anterograde and retrograde tracing to identify GABAergic connections between the MGB and IC. Previous research demonstrated increased spontaneous and burst activity levels in the external nucleus of the IC (ICx), a critical component of the auditory system, in animal models of tinnitus [31]. Additionally, noise exposure has been shown to alter neuronal excitability, indicative of neural plasticity [32]. Moreover, deep brain stimulation of the ICx can reduce tinnitus-like behaviors in rats. Our experimental results were aligned; specifically, retrograde tracing of the virus revealed that mCherry fluorescence was concentrated primarily in the ICx. Thus, future tinnitus experiments targeting the IC could consider the ICx substructure as a potential target.

The traditional view of tinnitus is that it arises from an excitation-inhibition imbalance caused by peripheral deafferentation inhibition. Reduced deafferent input in the auditory periphery leads to compensatory increases in excitability or synchronization in the central auditory pathway, enhanced self-gain, and self-remodeling (including tonotopic map reorganization and

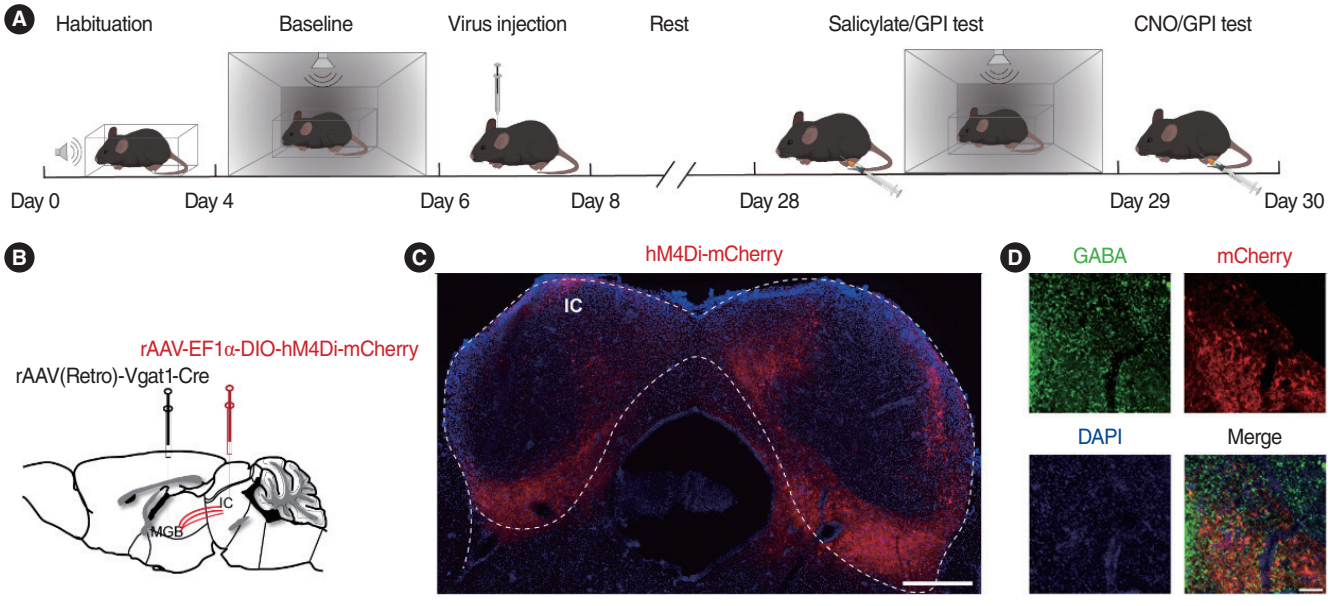

Fig. 5. Continued

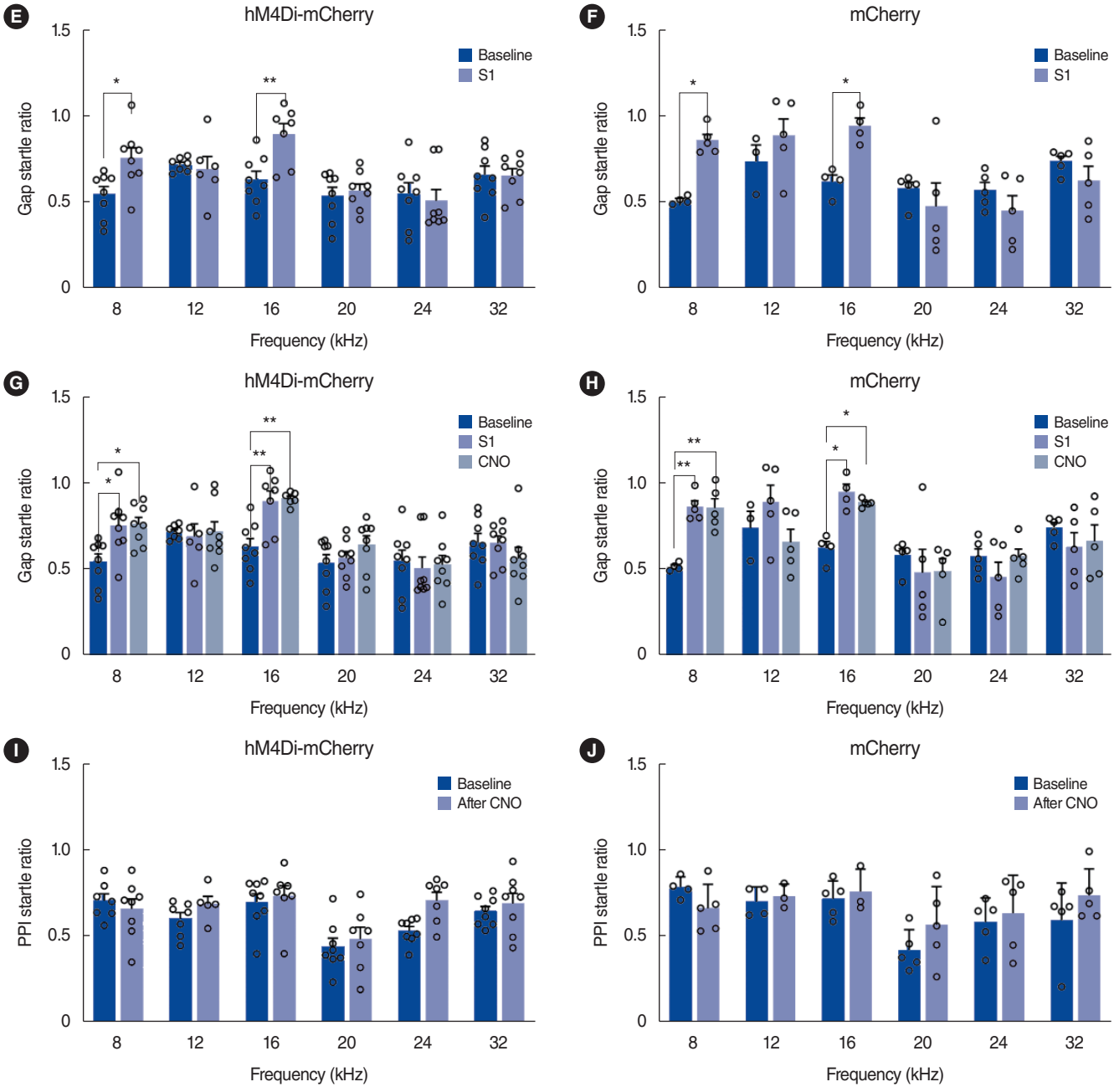

Fig. 5. Chemogenetic inhibition of IC^{GABA} neuron activity in the inferior colliculus (IC)-medial geniculate body (MGB) neural circuit in salicylate-induced tinnitus. (A) Timeline of the experiments. (B) Schematic illustration of viral injection for chemogenetic manipulation. (C) Representative image of mCherry-expressing neurons in the IC. Scale bar, 500 μm. (D) Characterization of mCherry-positive IC neurons; these neurons are reactive with gamma-aminobutyric acid (GABA)-specific antibody. Scale bars, 100 μm. (E, F) Gap startle ratios across various frequencies in mice injected with salicylate. (E) Column factor, F(1,80)=5.273, *P*=0.024; hM4Di-mCherry: 8 kHz, 95% CI: −0.412 to −0.009, *P*=0.036; 16 kHz, 95% CI: −0.472 to −0.055, *P*=0.006. (F) Column factor, F(1,43)=3.462, *P*=0.070; mCherry: 8 kHz, 95% CI: −0.644 to −0.052, *P*=0.014; 16 kHz, 95% CI: −0.637 to −0.013, *P*=0.037. (G, H) Gap startle ratios across various frequencies in mice injected with clozapine N-oxide (CNO). (G) Column factor, F(2,120)=4.119, *P*=0.019; hM4Di-mCherry: 8 kHz_baseline vs. 8 kHz_S1, 95% CI: −0.388 to −0.034, *P*=0.015; 8 kHz_baseline vs. 8 kHz_CNO, 95% CI: −0.393 to −0.039, *P*=0.012; 16 kHz_baseline vs. 16 kHz_S1, 95% CI: −0.446 to −0.080, *P*=0.003; 16 kHz_baseline vs. 16 kHz_CNO, 95% CI: −0.472 to −0.090, *P*=0.002. (H) Column factor, F(2,67)=1.899, *P*=0.158; mCherry: 8 kHz_baseline vs. 8 kHz_S1, 95% CI: −0.599 to −0.098, *P*=0.004; 8 kHz_baseline vs. 8 kHz_CNO, 95% CI: −0.590 to −0.090, *P*=0.005; 16 kHz_baseline vs. 16 kHz_S1, 95% CI: −0.589 to −0.061, *P*=0.012; 16 kHz_baseline vs. 16 kHz_CNO, 95% CI: −0.514 to −0.013, *P*=0.032. (I, J) Prepulse inhibition (PPI) startle ratios across various frequencies in mice. (I) PPI startle ratios of the hM4Di-mCherry group. (J) PPI startle ratios of the mCherry group. Values are presented as mean±standard error of the mean. **P*<0.05; ***P*<0.01 (two-way analysis of variance for E-J). hM4Di-mCherry, n=8 mice; mCherry, n=5 mice. GPI, gap prepulse inhibition; DAPI, 4′,6-diamidino-2-phenylindole; S1, salicylate day 1.

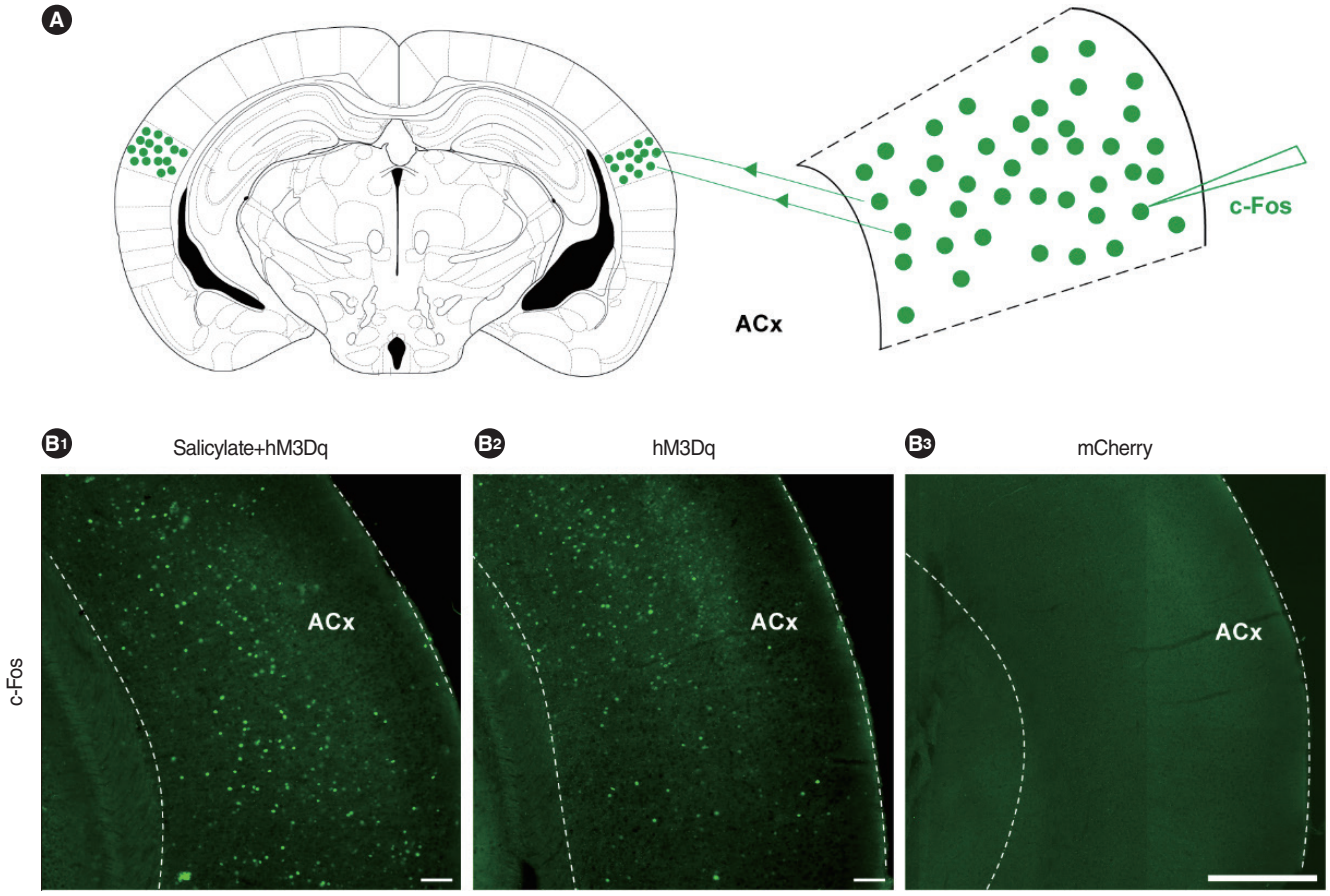

Fig. 6. Representative image of c-Fos–expressing neurons in the auditory cortex (ACx). (A) Schematic illustration of c-Fos in the ACx. (B) c-Fos expression in the ACx of mice with the inferior colliculus-medial geniculate body neural circuit expressing salicylate+hM3Dq/hM3Dq/mCherry following clozapine N-oxide injection. Scale bars, 200 μm (B1, B2), 500 μm (B3).

homeostatic plasticity) [33]. Concurrently, the downregulation of inhibitory transmitters in the DCN, IC, and ACx is thought to reflect altered homeostatic plasticity that compensates for reduced peripheral excitatory input [34]. However, the role of the MGB in tinnitus remains unclear. Whole-cell patch-clamp recording studies have indicated that approximately 80% of MGB neurons exhibit modified firing rates upon salicylate application, with 52.4% displaying increased activity and 47.6% showing decreased activity [35]. Kalappa et al. [17] reported increased spontaneous firing and bursting activity in the MGB units of tinnitus-exposed animals. Their study demonstrated that administering high concentrations of salicylate reduced MGB neuronal excitability, resulting in increased hyperpolarization of the resting potential [36]. In contrast, Barry et al. [37] did not observe significant changes in the spontaneous discharge rate of MGB neurons in response to noise exposure or tinnitus. Despite these contrasting findings, the consensus in the field suggests that alterations in the biological function of the MGB can trigger abnormal signaling along the auditory pathway, potentially contributing to the onset of tinnitus [38].

The results of our chemogenetic experiments revealed that activation of the IC-MGB GABAergic circuit effectively induced tinnitus. However, how the IC-MGB GABA neural circuit becomes activated in patients with tinnitus remains unclear. Stress conditions, such as sleep deprivation, excessive pressure, and mental strain, may trigger activation of the IC-MGB GABA pathway. Additionally, recent research indicates that patients with tinnitus exhibit changes in their gut microbiota, which could influence brain function via the gut-brain axis and contribute to the onset of tinnitus [39]; however, the exact mechanisms require further investigation.

The MGB contains numerous extrasynaptic receptors, among which extrasynaptic $GABA_A$ receptors ($GABA_ARs$) are activated by low GABA concentrations to mediate tonic and persistent inhibitory currents [40]. Caspary and Llano [41] found that rapid synaptic inhibition in the thalamus is mediated by GABA via synaptic $GABA_ARs$, while sustained tonic inhibition is mediated through high-affinity extrasynaptic $GABA_ARs$. Compared to other auditory structures, MGB circuits exhibit increased $GABA_AR$ function in animals with tinnitus, hyperpolarizing MGB neurons and inactivating T-type calcium channels [20]. MGB neurons subsequently generate slow calcium spikes, leading to

low-frequency repetitive interactions between the auditory thalamus and cortex and resulting in abnormal cortical oscillations. This mechanism aligns with the TCD hypothesis, believed to underlie tinnitus perception [12,42,43]. In this study, we activated GABAergic neurons in the MGB, increasing GABA release. This increased GABA binding to $GABA_A$Rs triggered the hyperpolarization of MGB neurons, supporting the TCD hypothesis.

Abnormal brain activity characterized by heightened gamma rhythms and diminished alpha rhythms has been observed in the auditory areas of patients with tinnitus [42]. TCD arises due to reduced inhibitory inputs to adjacent cortical regions, and this reduction in inhibition promotes activity within the neighboring disinhibitory cortex, ultimately resulting in a sustained increase in high-frequency activity (>30 Hz) in the gamma region [43]. Spectral analysis of brain activity in an animal model of salicylate-induced tinnitus has revealed significantly decreased alpha-wave activity and increased gamma-wave activity within the ACx region [44]. This finding also explains why further activation of IC-MGB GABAergic pathways, combined with salicylate treatment, exacerbates the severity of tinnitus. The synergistic effect further amplifies gamma-band activity in the ACx. Nevertheless, our activation experiments did not clarify whether hyperpolarization was mediated through synaptic, extrasynaptic, or even external inhibitory sources outside the thalamus.

Unlike activation, inhibition of the IC^{GABA}-MGB circuit did not reduce or alleviate tinnitus. These findings suggest that the mechanism underlying tinnitus perception induced by the IC^{GABA}-MGB pathway differs from that of salicylate-induced tinnitus. In addition to the traditional auditory pathways, other nuclei or neural circuits may also contribute to the modulation of tinnitus. Animal studies have shown increased metabolic activity in the medial prefrontal cortex during tinnitus [45]. This region is crucial for sensory gating, primarily via an indirect pathway connecting the TRN to the MGB [46]. Resting-state functional magnetic resonance imaging studies have identified structural and functional abnormalities in the nucleus accumbens associated with tinnitus; this region is more active than other brain structures (e.g., the ACx) when patients perceive tinnitus-like sounds [47]. Additional studies have revealed altered connectivity between the hippocampus and other brain regions in individuals with tinnitus [48], resulting in a stronger link between the auditory system and the hippocampus [49]. Additionally, abnormal interactions between the auditory pathway and the amygdala could influence the emotional aspects of tinnitus [50].

However, as previously discussed, the mechanism by which the IC-MGB pathway produces tinnitus involves activation effects on IC, MGB, and GABAergic neurons. This induction is singular, the neural nuclei involved are fixed, and the precise mechanism remains unclear. Thus, in mice with salicylate-induced tinnitus, activation of this neural circuit due to overlapping induction mechanisms can exacerbate tinnitus symptoms. In contrast, inhibition of this neural circuit did not reduce or provide therapeutic relief for tinnitus due to the diverse mechanisms by which salicylate induces tinnitus. Additionally, partial viral expression efficiency or incomplete neuronal silencing may have limited the magnitude of observed effects, potentially contributing to the lack of statistical significance regarding the inhibition of IC-MGB GABAergic neurons. Future studies will thus require complementary approaches to clarify the causal role of complete IC-MGB pathway silencing in tinnitus pathology.

Although our research has made initial progress in investigating the role of IC-MGB GABAergic neural circuits in tinnitus, several limitations remain. First, we primarily focused on observations and descriptions at a phenomenological level. Notably, increased c-Fos expression in the ACx is commonly interpreted as indicative of neural activation. Importantly, however, c-Fos serves as a general marker of neuronal activity rather than a specific indicator of tinnitus perception. Future studies should employ more refined and diverse technical methods, such as *in vivo* electrophysiological recordings and patch-clamp techniques, to more thoroughly reveal the functions and mechanisms of this neural circuit. Second, deeper exploration of the dynamic changes in neurotransmitters, modulatory factors, and small molecules in the IC-MGB neural circuits is needed to clarify their roles in tinnitus onset and progression. Third, our study specifically utilized the salicylate-induced tinnitus model, limiting the generalizability of the findings to other models. Despite these constraints, the widespread use, reversibility, and dose controllability of the salicylate-induced model provide valuable insights into specific mechanisms. Future studies should validate these findings using other tinnitus models, such as those induced by noise exposure. Finally, our discussion of the MGB's role in tinnitus was limited to TCD, which does not sufficiently explain all pathological features of tinnitus. Therefore, future research should explore the MGB gating mechanism hypothesis.

In conclusion, our study identified the IC-MGB GABAergic neural circuit as playing an important role in the induction—but not the suppression—of tinnitus, providing new insights into its underlying mechanisms. These insights could potentially lead to groundbreaking methods for identifying therapeutic neurotargets for tinnitus management.

CONFLICT OF INTEREST

No potential conflict of interest relevant to this article was reported.

ACKNOWLEDGMENTS

This research was supported by the National Natural Science Foundation (82071061 and 32271059), the Young Scholars Fostering Fund of the First Affiliated Hospital with Nanjing Medical

University (PY202422), and the Jiangsu Province Capability Improvement Project through Science, Technology and Education (JSDW202203) of China.

ORCID

Xu-Yuan Peng https://orcid.org/0009-0008-1184-5988
Jiang Wang https://orcid.org/0000-0001-6597-5501
Ming-Yue Gong https://orcid.org/0009-0001-4232-4025
Li-Yuan Zhang https://orcid.org/0000-0002-6117-4384
Min Zhang https://orcid.org/0000-0001-5357-6773
Zhi-Bin Chen https://orcid.org/0000-0003-2548-0576
Zheng-Quan Tang https://orcid.org/0000-0003-1691-6358
Lei Cheng https://orcid.org/0000-0001-6541-7702

AUTHOR CONTRIBUTIONS

Conceptualization: ZQT, LC. Methodology: XYP, JW, MYG. Formal analysis: XYP, MYG, LYZ. Data curation: MYG, MZ. Visualization: ZBC. Project administration: JW, LC. Funding acquisition: JW, ZQT, LC. Writing–original draft: XYP, JW, MYG. Writing–review & editing: ZQT, LC. All authors read and agreed to the published version of the manuscript.

SUPPLEMENTARY MATERIALS

Supplementary materials can be found online at https://doi.org/10.21053/ceo.2025-00027.

REFERENCES

1. Piccirillo JF, Rodebaugh TL, Lenze EJ. Tinnitus. JAMA. 2020 Apr;323(15):1497-8.
2. Clifford RE, Maihofer AX, Chatzinakos C, Coleman JR, Daskalakis NP, Gasperi M, et al. Genetic architecture distinguishes tinnitus from hearing loss. Nat Commun. 2024 Jan;15(1):614.
3. Langguth B, Kreuzer PM, Kleinjung T, De Ridder D. Tinnitus: causes and clinical management. Lancet Neurol. 2013 Sep;12(9):920-30.
4. Hall DA, Fackrell K, Li AB, Thavayogan R, Smith S, Kennedy V, et al. A narrative synthesis of research evidence for tinnitus-related complaints as reported by patients and their significant others. Health Qual Life Outcomes. 2018 Apr;16(1):61.
5. Simoes JP, Daoud E, Shabbir M, Amanat S, Assouly K, Biswas R, et al. Multidisciplinary tinnitus research: challenges and future directions from the perspective of early stage researchers. Front Aging Neurosci. 2021 Jun;13:647285.
6. Eggermont JJ, Roberts LE. The neuroscience of tinnitus. Trends Neurosci. 2004 Nov;27(11):676-82.
7. Li S, Choi V, Tzounopoulos T. Pathogenic plasticity of Kv7.2/3 channel activity is essential for the induction of tinnitus. Proc Natl Acad Sci U S A. 2013 Jun;110(24):9980-5.
8. Brozoski TJ, Wisner KW, Sybert LT, Bauer CA. Bilateral dorsal cochlear nucleus lesions prevent acoustic-trauma induced tinnitus in an animal model. J Assoc Res Otolaryngol. 2012 Feb;13(1):55-66.
9. Tan HT, Smith PF, Zheng Y. Time-dependent effects of acoustic trauma and tinnitus on extracellular levels of amino acids in the inferior colliculus of rats. Hear Res. 2024 Mar;443:108948.
10. Bartlett EL. The organization and physiology of the auditory thalamus and its role in processing acoustic features important for speech perception. Brain Lang. 2013 Jul;126(1):29-48.
11. Henton A, Tzounopoulos T. What's the buzz?: the neuroscience and the treatment of tinnitus. Physiol Rev. 2021 Oct;101(4):1609-32.
12. Gunbey HP, Gunbey E, Aslan K, Bulut T, Unal A, Incesu L. Limbic-auditory interactions of tinnitus: an evaluation using diffusion tensor imaging. Clin Neuroradiol. 2017 Jun;27(2):221-30.
13. Almasabi F, van Zwieten G, Alosaimi F, Smit JV, Temel Y, Janssen ML, et al. The effect of noise trauma and deep brain stimulation of the medial geniculate body on tissue activity in the auditory pathway. Brain Sci. 2022 Aug;12(8):1099.
14. van Zwieten G, Janssen ML, Smit JV, Janssen AM, Roet M, Jahanshahi A, et al. Inhibition of experimental tinnitus with high frequency stimulation of the rat medial geniculate body. Neuromodulation. 2019 Jun;22(4):416-24.
15. Fujimoto H, Notsu E, Yamamoto R, Ono M, Hioki H, Takahashi M, et al. Kv4.2-positive domains on dendrites in the mouse medial geniculate body receive ascending excitatory and inhibitory inputs preferentially from the inferior colliculus. Front Neurosci. 2021 Sep;15:740378.
16. Cope DW, Di Giovanni G, Fyson SJ, Orbán G, Errington AC, Lorincz ML, et al. Enhanced tonic GABAA inhibition in typical absence epilepsy. Nat Med. 2009 Dec;15(12):1392-8.
17. Kalappa BI, Brozoski TJ, Turner JG, Caspary DM. Single unit hyperactivity and bursting in the auditory thalamus of awake rats directly correlates with behavioural evidence of tinnitus. J Physiol. 2014 Nov;592(22):5065-78.
18. Su YY, Luo B, Jin Y, Wu SH, Lobarinas E, Salvi RJ, et al. Altered neuronal intrinsic properties and reduced synaptic transmission of the rat's medial geniculate body in salicylate-induced tinnitus. PLoS One. 2012;7(10):e46969.
19. Berlot E, Arts R, Smit J, George E, Gulban OF, Moerel M, et al. A 7 Tesla fMRI investigation of human tinnitus percept in cortical and subcortical auditory areas. Neuroimage Clin. 2020;25:102166.
20. Sametsky EA, Turner JG, Larsen D, Ling L, Caspary DM. Enhanced GABAA-mediated tonic inhibition in auditory thalamus of rats with behavioral evidence of tinnitus. J Neurosci. 2015 Jun;35(25):9369-80.
21. Beebe NL, Mellott JG, Schofield BR. Inhibitory projections from the inferior colliculus to the medial geniculate body originate from four subtypes of GABAergic cells. eNeuro. 2018 Nov;5(5):ENEURO.0406-18.2018.
22. Pavlidis P, Papadopoulou K, Tseriotis VS, Karachrysafi S, Sardeli C, Gouveris H, et al. Salicylate- and Noise-induced tinnitus: different mechanisms producing the same result?: an experimental model. Indian J Otolaryngol Head Neck Surg. 2023 Dec;75(4):3535-44.
23. Noreña AJ. An integrative model of tinnitus based on a central gain controlling neural sensitivity. Neurosci Biobehav Rev. 2011 Apr;35(5):1089-109.
24. Sheppard A, Hayes SH, Chen GD, Ralli M, Salvi R. Review of salicylate-induced hearing loss, neurotoxicity, tinnitus and neuropathophysiology. Acta Otorhinolaryngol Ital. 2014 Apr;34(2):79-93.
25. Pienkowski M, Ulfendahl M. Differential effects of salicylate, quinine, and furosemide on Guinea pig inner and outer hair cell function revealed by the input-output relation of the auditory brainstem response. J Am Acad Audiol. 2011 Feb;22(2):104-12.
26. Song A, Cho GW, Moon C, Park I, Jang CH. Protective effect of resveratrol in an experimental model of salicylate-induced tinnitus. Int J Mol Sci. 2022 Nov;23(22):14183.

27. Wang HT, Luo B, Zhou KQ, Xu TL, Chen L. Sodium salicylate reduces inhibitory postsynaptic currents in neurons of rat auditory cortex. Hear Res. 2006 May;215(1-2):77-83.
28. Jastreboff PJ, Brennan JF, Coleman JK, Sasaki CT. Phantom auditory sensation in rats: an animal model for tinnitus. Behav Neurosci. 1988 Dec;102(6):811-22.
29. Ralli M, Lobarinas E, Fetoni AR, Stolzberg D, Paludetti G, Salvi R. Comparison of salicylate- and quinine-induced tinnitus in rats: development, time course, and evaluation of audiologic correlates. Otol Neurotol. 2010 Jul;31(5):823-31.
30. Zhao J, Wang B, Wang X, Shang X. Up-regulation of Ca/CaMKII/CREB signaling in salicylate-induced tinnitus in rats. Mol Cell Biochem. 2018 Nov;448(1-2):71-6.
31. Chen GD, Jastreboff PJ. Salicylate-induced abnormal activity in the inferior colliculus of rats. Hear Res. 1995 Feb;82(2):158-78.
32. Szczepaniak WS, Møller AR. Evidence of neuronal plasticity within the inferior colliculus after noise exposure: a study of evoked potentials in the rat. Electroencephalogr Clin Neurophysiol. 1996 Mar;100(2):158-64.
33. Eggermont JJ. Tinnitus: neurobiological substrates. Drug Discov Today. 2005 Oct;10(19):1283-90.
34. Pilati N, Ison MJ, Barker M, Mulheran M, Large CH, Forsythe ID, et al. Mechanisms contributing to central excitability changes during hearing loss. Proc Natl Acad Sci U S A. 2012 May;109(21):8292-7.
35. Basta D, Goetze R, Ernst A. Effects of salicylate application on the spontaneous activity in brain slices of the mouse cochlear nucleus, medial geniculate body and primary auditory cortex. Hear Res. 2008 Jun;240(1-2):42-51.
36. Wang XX, Jin Y, Luo B, Sun JW, Zhang J, Wang M, et al. Sodium salicylate potentiates the GABAB-GIRK pathway to suppress rebound depolarization in neurons of the rat's medial geniculate body. Hear Res. 2016 Feb;332:104-12.
37. Barry KM, Robertson D, Mulders WH. Changes in auditory thalamus neural firing patterns after acoustic trauma in rats. Hear Res. 2019 Aug;379:89-97.
38. Liu P, Xue X, Zhang C, Zhou H, Ding Z, Wang L, et al. Transcriptional-profile changes in the medial geniculate body after noise-induced tinnitus. Exp Biol Med (Maywood). 2024 Mar;249:10057.
39. Wang J, Xiang JH, Peng XY, Liu M, Sun LJ, Zhang M, et al. Characteristic alterations of gut microbiota and serum metabolites in patients with chronic tinnitus: a multi-omics analysis. Microbiol Spectr. 2025 Jan;13(1):e0187824.
40. Richardson BD, Brozoski TJ, Ling LL, Caspary DM. Targeting inhibitory neurotransmission in tinnitus. Brain Res. 2012 Nov;1485:77-87.
41. Caspary DM, Llano DA. Auditory thalamic circuits and GABA receptor function: putative mechanisms in tinnitus pathology. Hear Res. 2017 Jun;349:197-207.
42. De Ridder D, Vanneste S, Langguth B, Llinas R. Thalamocortical dysrhythmia: a theoretical update in tinnitus. Front Neurol. 2015 Jun;6:124.
43. Llinás R, Urbano FJ, Leznik E, Ramírez RR, van Marle HJ. Rhythmic and dysrhythmic thalamocortical dynamics: GABA systems and the edge effect. Trends Neurosci. 2005 Jun;28(6):325-33.
44. Singh A, Smith PF, Zheng Y. Targeting the limbic system: insights into its involvement in tinnitus. Int J Mol Sci. 2023 Jun;24(12):9889.
45. Wu C, Bao W, Yi B, Wang Q, Wu X, Qian M, et al. Increased metabolic activity and hysteretic enhanced GABA receptor binding in a rat model of salicylate-induced tinnitus. Behav Brain Res. 2019 May;364:348-55.
46. Nakajima M, Schmitt LI, Halassa MM. Prefrontal cortex regulates sensory filtering through a basal ganglia-to-thalamus pathway. Neuron. 2019 Aug;103(3):445-58.e10.
47. Rauschecker JP, May ES, Maudoux A, Ploner M. Frontostriatal gating of tinnitus and chronic pain. Trends Cogn Sci. 2015 Oct;19(10):567-78.
48. Mohan A, Davidson C, De Ridder D, Vanneste S. Effective connectivity analysis of inter- and intramodular hubs in phantom sound perception - identifying the core distress network. Brain Imaging Behav. 2020 Feb;14(1):289-307.
49. Chen YC, Li X, Liu L, Wang J, Lu CQ, Yang M, et al. Tinnitus and hyperacusis involve hyperactivity and enhanced connectivity in auditory-limbic-arousal-cerebellar network. Elife. 2015 May;4:e06576.
50. Crippa A, Lanting CP, van Dijk P, Roerdink JB. A diffusion tensor imaging study on the auditory system and tinnitus. Open Neuroimag J. 2010 Jun;4:16-25.